Exploring Active Galactic Nuclei with LST-1

Lea Heckmann

Credit: Irene Burelli

Credit

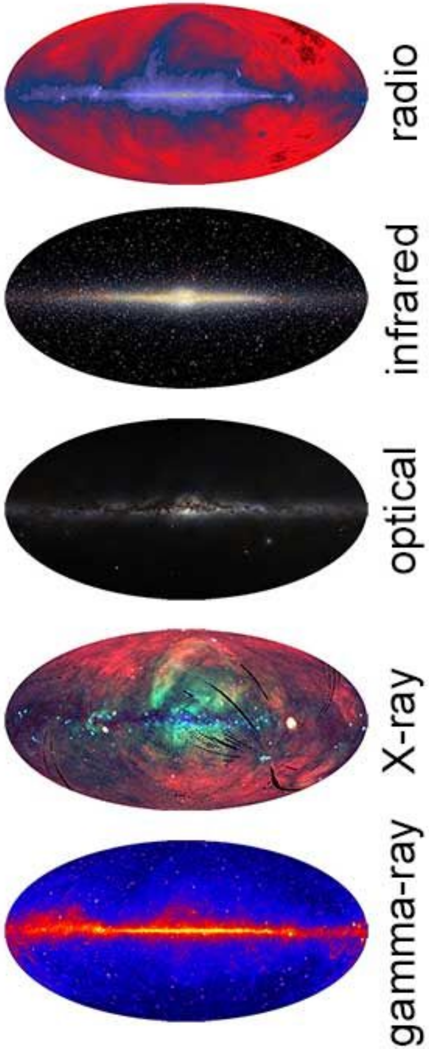

Credit: NASA

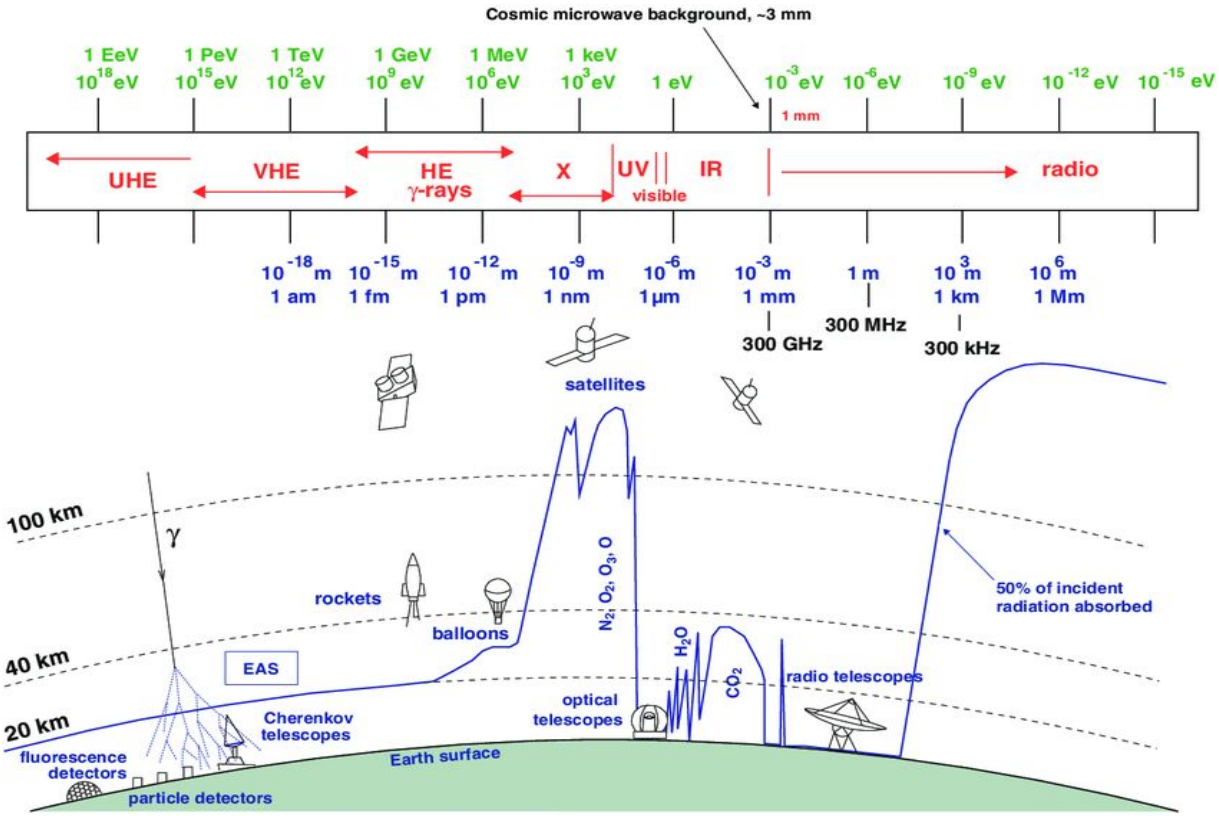

Credit: Longair, S. M. (1992)

Exploring new horizons in the VHE regime

- Cherenkov Telescope Array Observatory (CTAO)
    - Northern + Southern array
    - Improved sensitivity & increased energy range in VHE

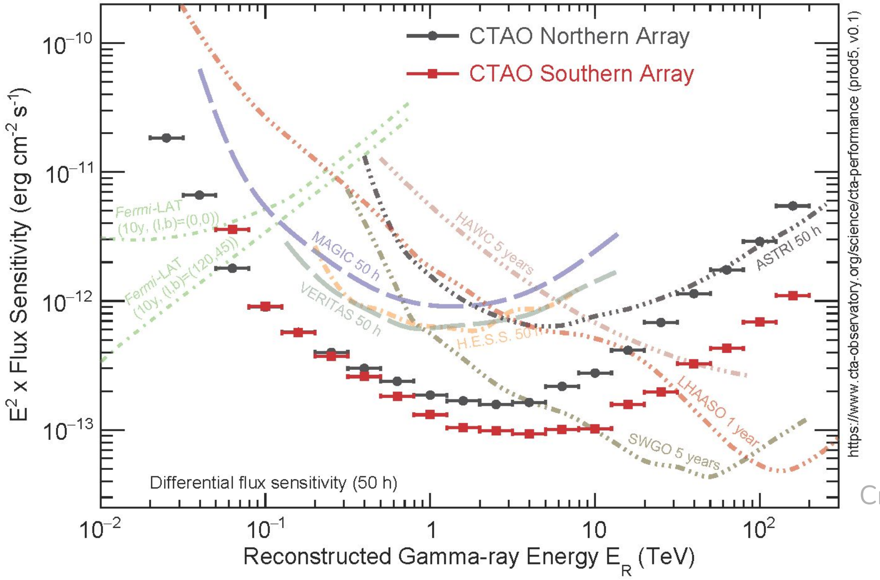

Credit: CTAO

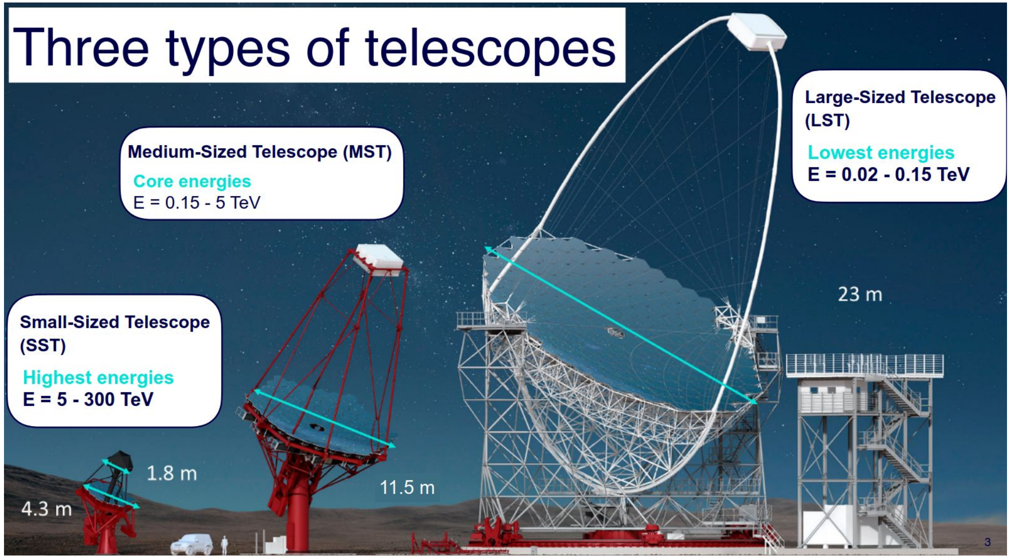

Adapted from A. López Oramas, 2nd VHEGAM 2025

Exploring new horizons in the VHE regime

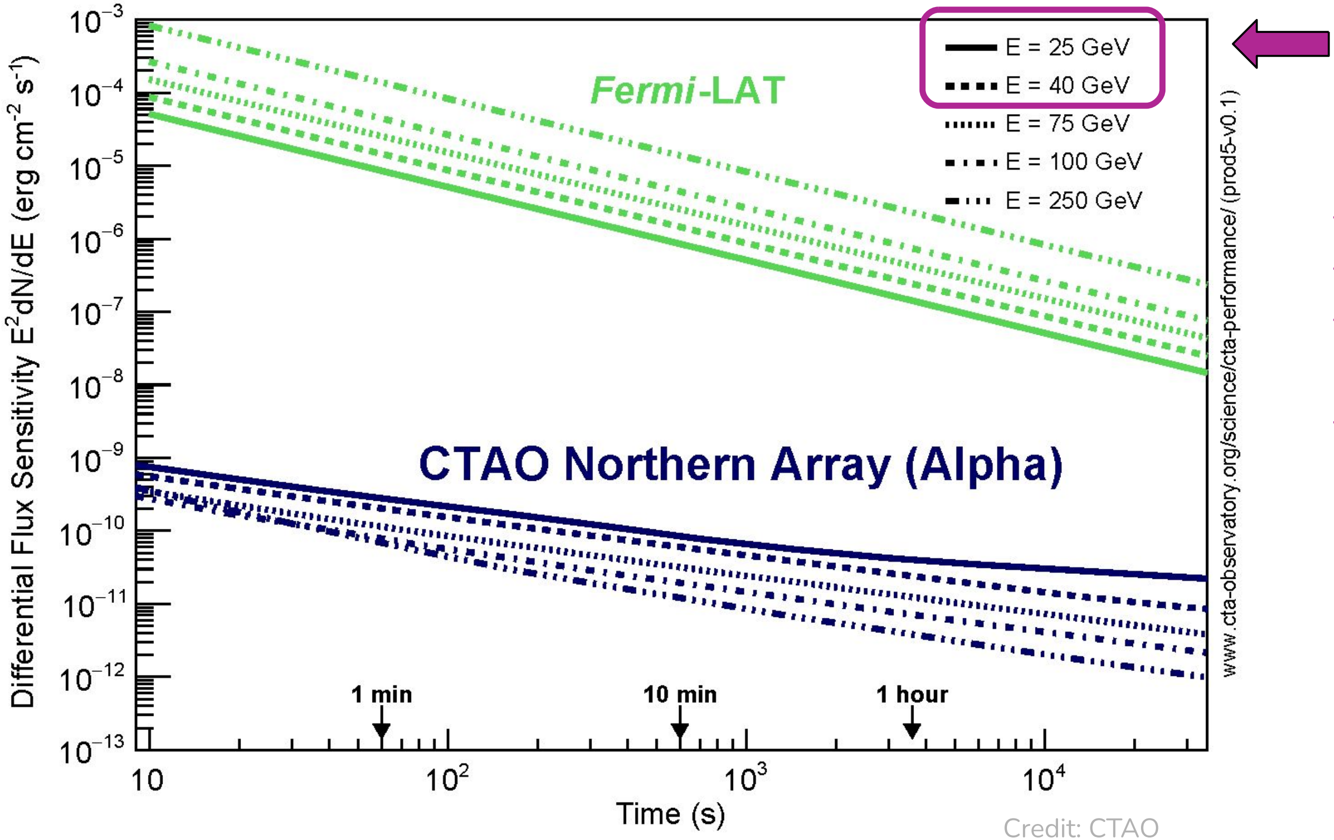

Credit: CTAO

LSTs dominate the sensitivity

- → **transient studies**
- → **cosmological sources**
- → **high redshift sources**
- → **pulsars**

Exploring new horizons in the VHE regime

- LST-1
  - Large-Sized Telescope prototype on La Palma
  - Improves energy threshold to ~20 GeV
  - Since 2018 in commissioning
  - Since ~2020 performing regular observations of different astrophysical source
- LST 2-4
  - The rest of the Northern array
  - Being constructed at the moment
- LST 5-6
  - Southern array
  - Being planned at the moment

Credit: CTAO

The extragalactic sky with LST-1

- >1000 hours of data taken on extragalactic objects
- Started with previously know TeV blazars during early-commissioning

AGN Zoo K. Abe et al, MNRAS 544, 1, 669–686 (2025)

- Mini-catalog of bright BL Lacs (z=0.03 to 0.5)
  - Mrk 421
  - Mrk 501
  - 1ES 1959+650
  - 1ES 0647+250
  - PG 1553 + 113
- Commissioning data from 2020-2022
- Variability study identification of emission states

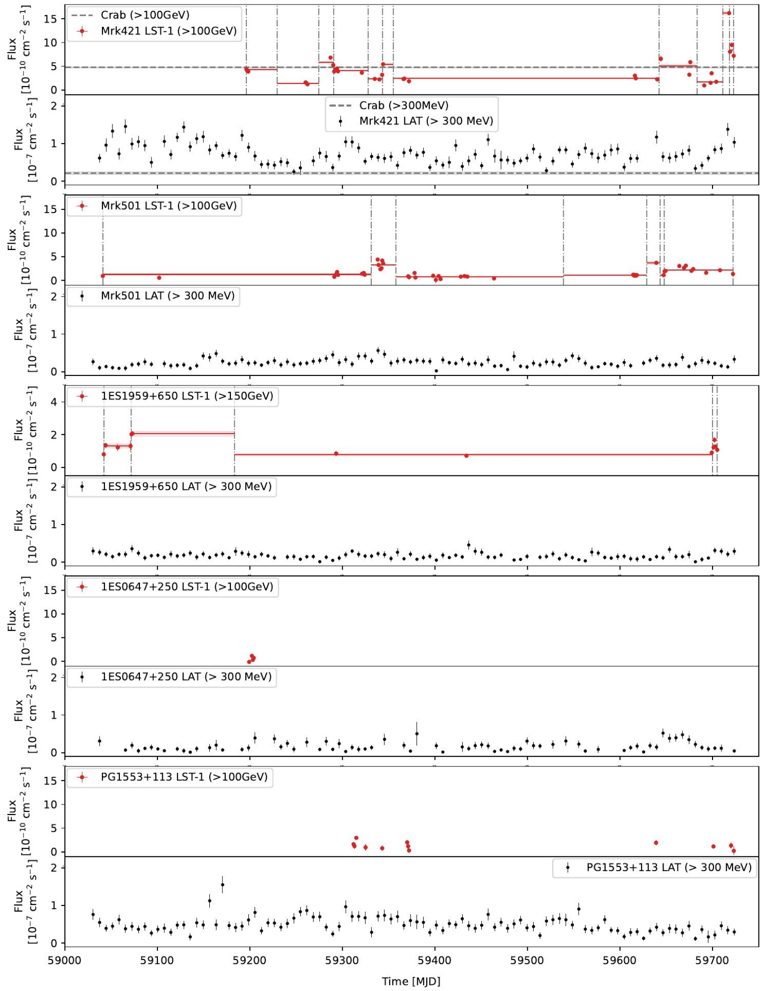

AGN Zoo

K. Abe et al, MNRAS 544, 1, 669–686 (2025)

- Mini-catalog of bright BL Lacs (z=0.03 to 0.5)
  - Mrk 421
  - Mrk 501
  - 1ES 1959+650
  - 1ES 0647+250
  - PG 1553 + 113
- Commissioning data from 2020-2022
- Variability study identification of emission states
  - Intra-night variability detected in one night for Mrk 421

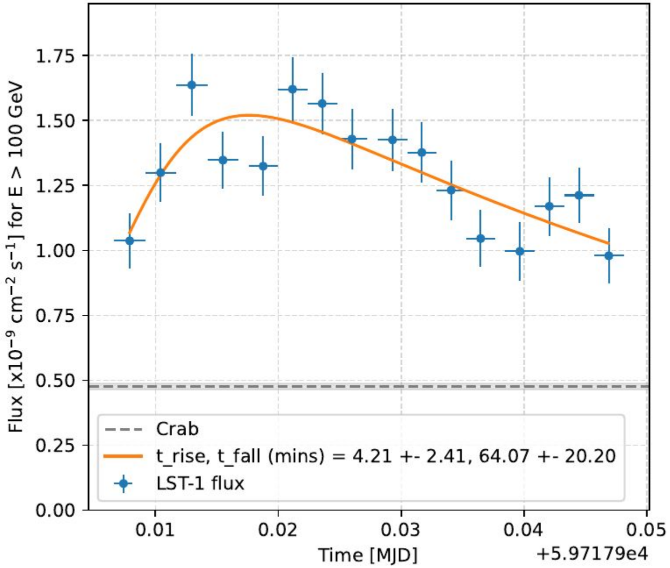

AGN Zoo K. Abe et al, MNRAS 544, 1, 669–686 (2025)

- Identification of emission states in VHE and HE gamma-rays (Bayesian blocks)
- Joint LST-1 and Fermi-LAT fits of various emission states (asgardpy)

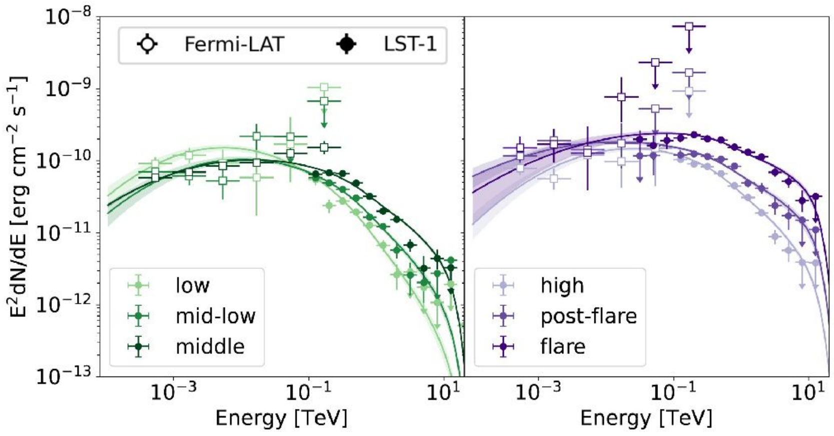

(a) Mrk 421

AGN Zoo

K. Abe et al, MNRAS 544, 1, 669–686 (2025)

- Identification of emission states in VHE and HE gamma-rays (Bayesian blocks)

- Joint LST-1 and Fermi-LAT fits of various emission states (asgardpy)

  - Spectral indices (2.0 - 2.4) are in line with shock acceleration for all sources

  - Peak energies of Mrk 421 increase with flux states → acceleration becoming more efficient

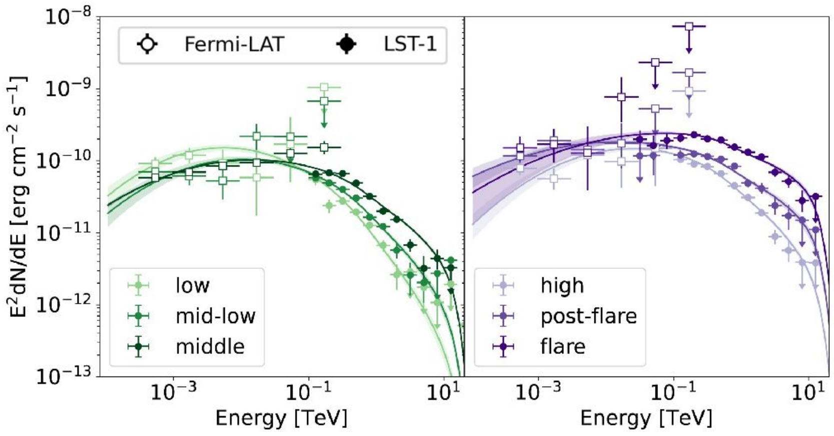

(a) Mrk 421

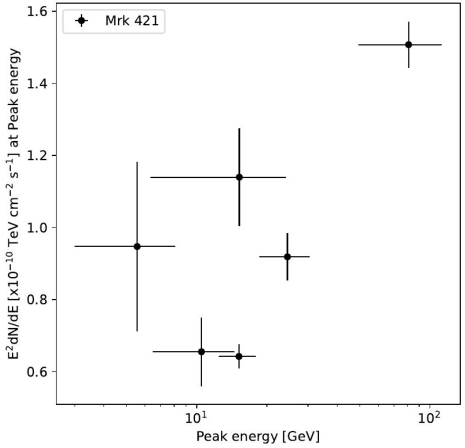

AGN Zoo K. Abe et al, MNRAS 544, 1, 669–686 (2025)

- Blazar detectability study:
  Simulation of various GeV/TeV flares at different red-shifts
  (10 hours of observation at culmination for each source)

  → Detectability of exceptional flare until z=1.2 for LST-1

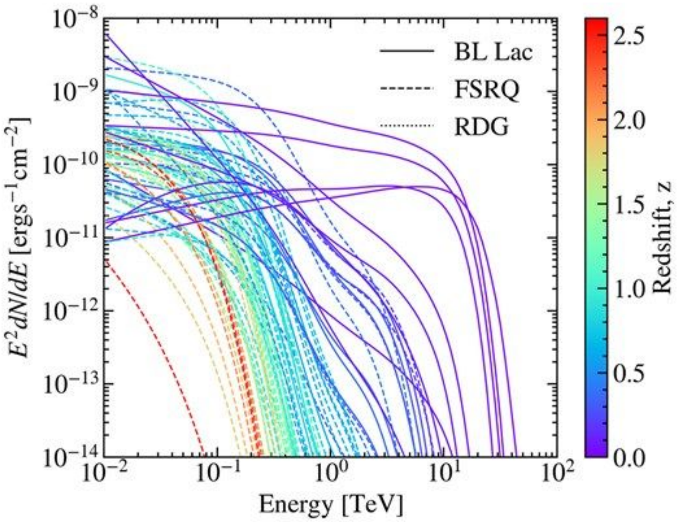

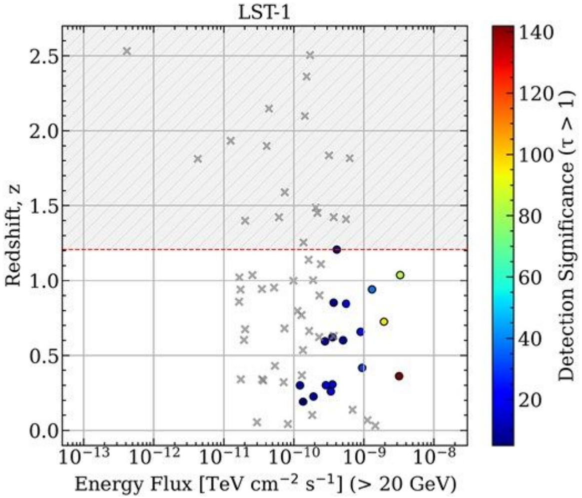

AGN Zoo

K. Abe et al, MNRAS 544, 1, 669–686 (2025)

- Blazar detectability study:
  Simulation of various GeV/TeV flares at different red-shifts
  (10 hours of observation at culmination for each source)

  → Detectability of exceptional flare until z=1.2 for LST-1

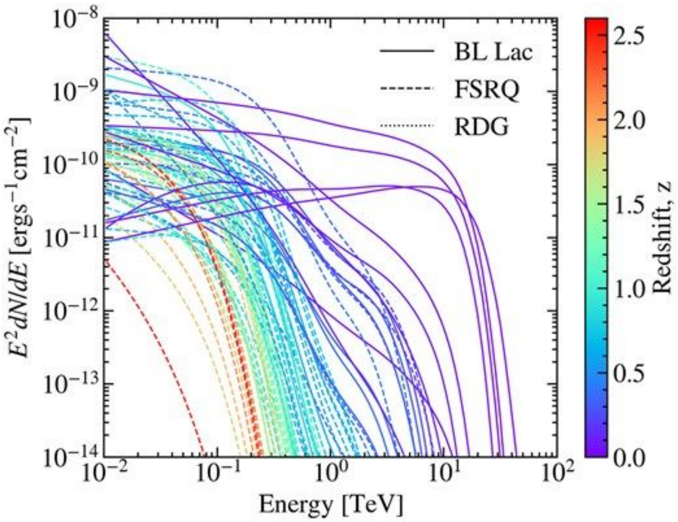

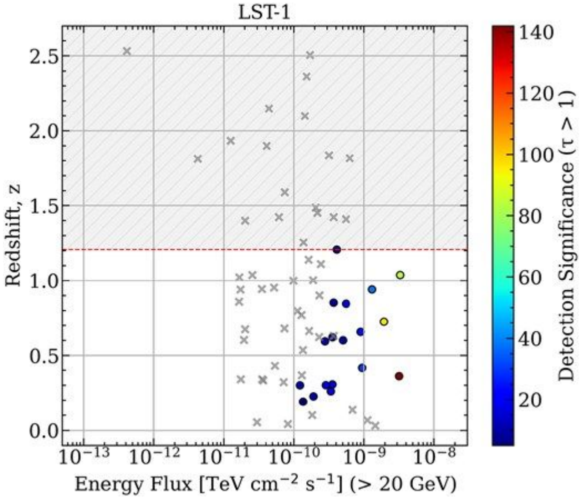


R. Takeishi


C. Priyadarshi


L. Heckmann


M. Nievas Rosillo


J. Baxter

The extragalactic sky with LST-1

- >1000 hours of data taken on extragalactic objects
- Started with previously know TeV blazars during early-commissioning

The extragalactic sky with LST-1

- >1000 hours of data taken on extragalactic objects
- Started with previously know TeV blazars during early-commissioning
- Strong ToO program based on
  - Fermi-LAT alerts:
    - Daily automatic light curve analysis (FlaapLUC; J.-P. Lenain, 2017)
    - Cluster of high-energy photons (Flaschep; S. Nozaki)
  - Optical flux alerts (ZTF; M. Nievas Rosillo)
  - Other external channels (Atels,...)

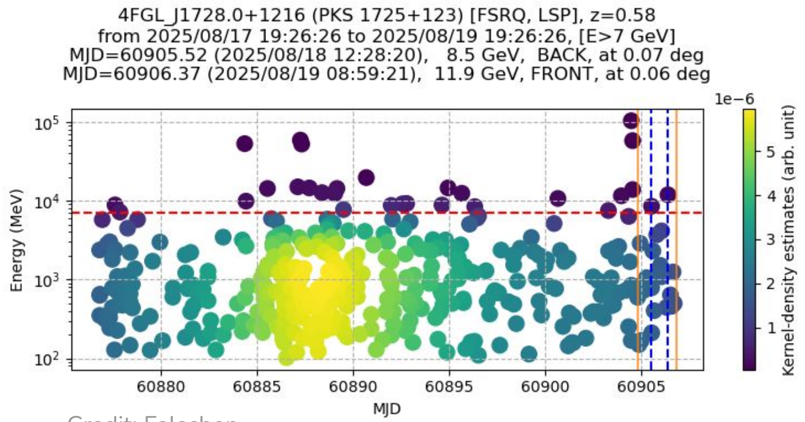

Credit: Falschep

The extragalactic sky with LST-1

- >1000 hours of data taken on extragalactic objects

- Started with previously know TeV blazars during early-commissioning

- Strong ToO program based on
  - Fermi-LAT alerts:
    - Daily automatic light curve analysis (FlaapLUC; J.-P. Lenain, 2017)
    - Cluster of high-energy photons (Flaschep; S. Nozaki)
  - Optical flux alerts (ZTF; M. Nievas Rosillo)
  - Other external channels (Atels,...)

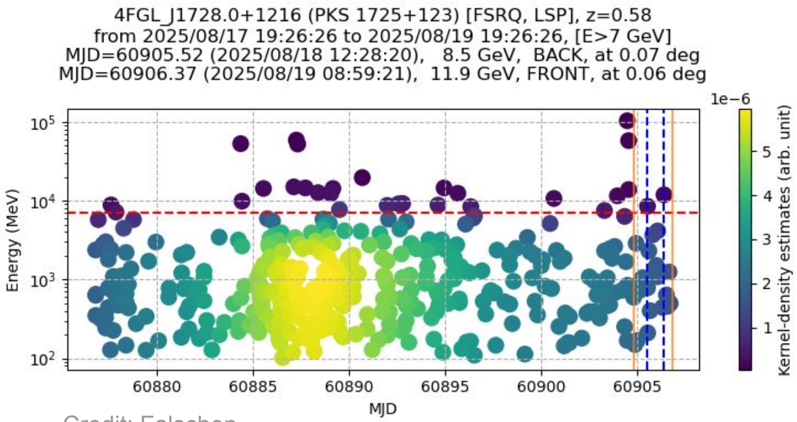

Credit: Falschep

- Now exploiting more the strength of LST-1:

  - Low energy-threshold -> high-redshift sources

  - Combination with MAGIC telescopes
    - Optimize Science return in the pre-CTAO era
    - Better sensitivity in the medium energy ranges with the three telescopes

BL Lacertae

- Only detected in VHE during flares
- Several flare detected in the past

- Two of the brightest outburst in VHE caught by LST-1 (2021, 2022)

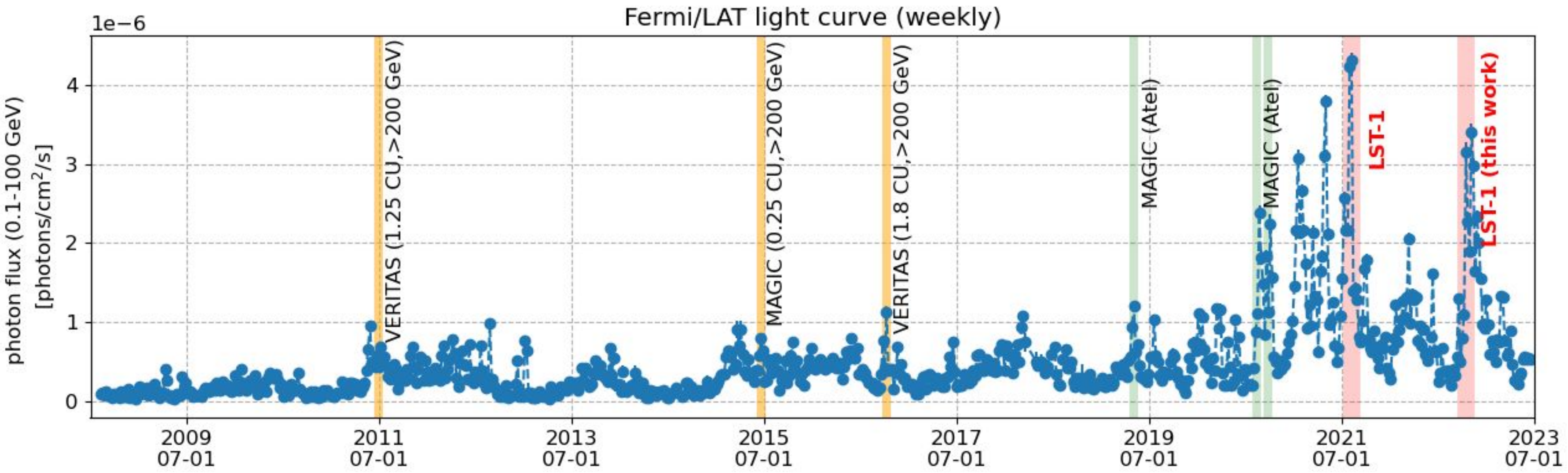

Adapted from S. Nozaki and J. Otero-Santos

BL Lacertae 2022 flare K. Abe et al, A&A, 710, A41 (2026)

- Flare in VHE & HE gamma-rays accompanied by variability patterns in other wavebands

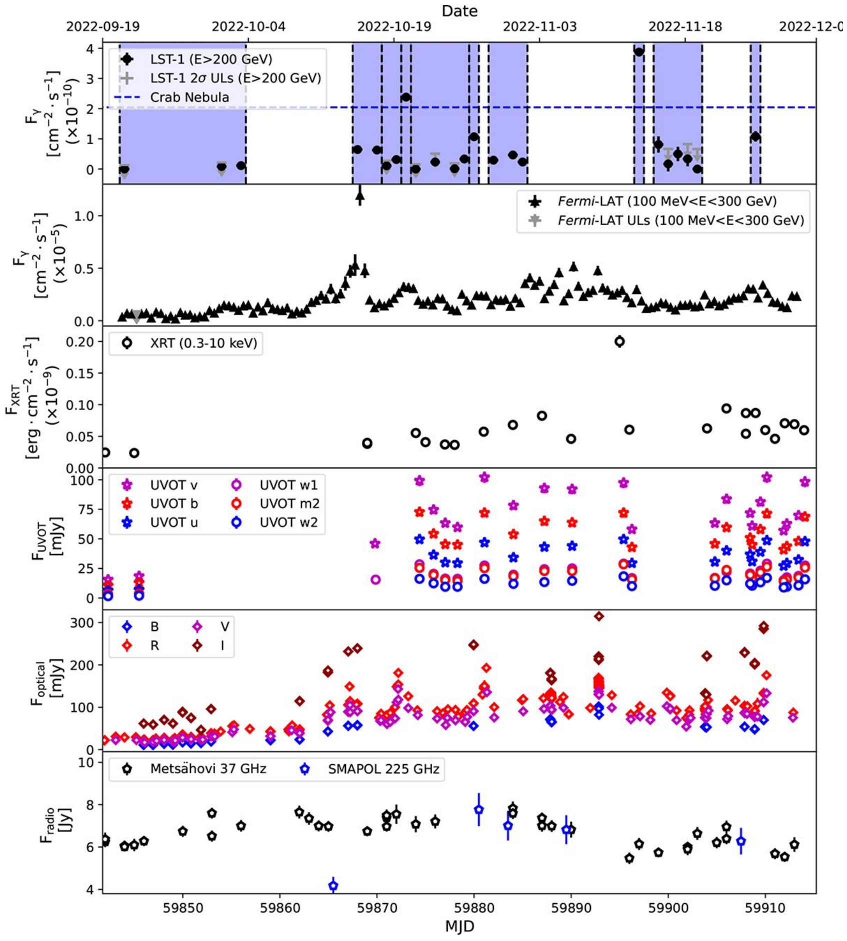

BL Lacertae 2022 flare

K. Abe et al, A&A, 710, A41 (2026)

- Flare in VHE & HE gamma-rays accompanied by variability patterns in other wavebands

- Internight variability
  - Brightest nights: 20 Oct and 13 Nov
  - Exponential rise & decay:
    20 Oct: ~18 min >5σ and hints between 2.2-4.6 min ~2σ
  - Flux doubling time scales:
    Oct 20: 8.3 ± 2.5 min >3σ before trials

→R ≤ (1.4 ± 0.4) to (7.0 ± 2.1) × 10^{14} cm (δ = 10–50)

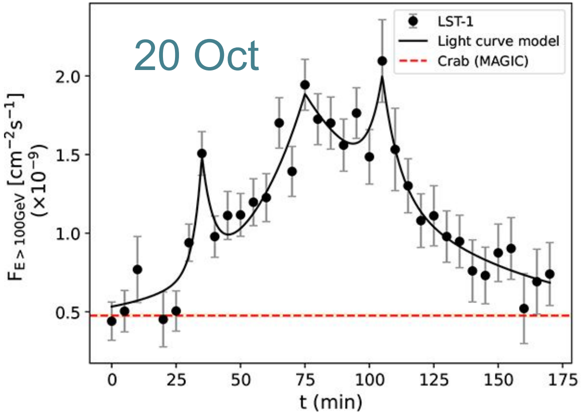

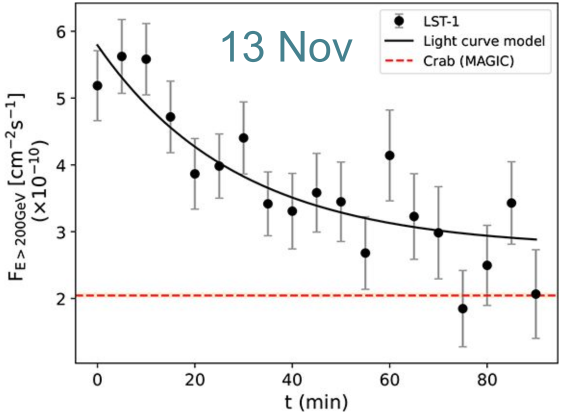

BL Lacertae 2022 flare
K. Abe et al, A&A, 710, A41 (2026)

- Time-dependent modelling
  - 10 broadband SEDS identified bt Bayesian blocks
  - Leptonic scenarios (favored by IXPE results, I. Agudo et al. 2025)
    - One zone insufficient (SSC or EC) → Two-zone scenario with interaction
      - “Core” zone > “Blob” zone

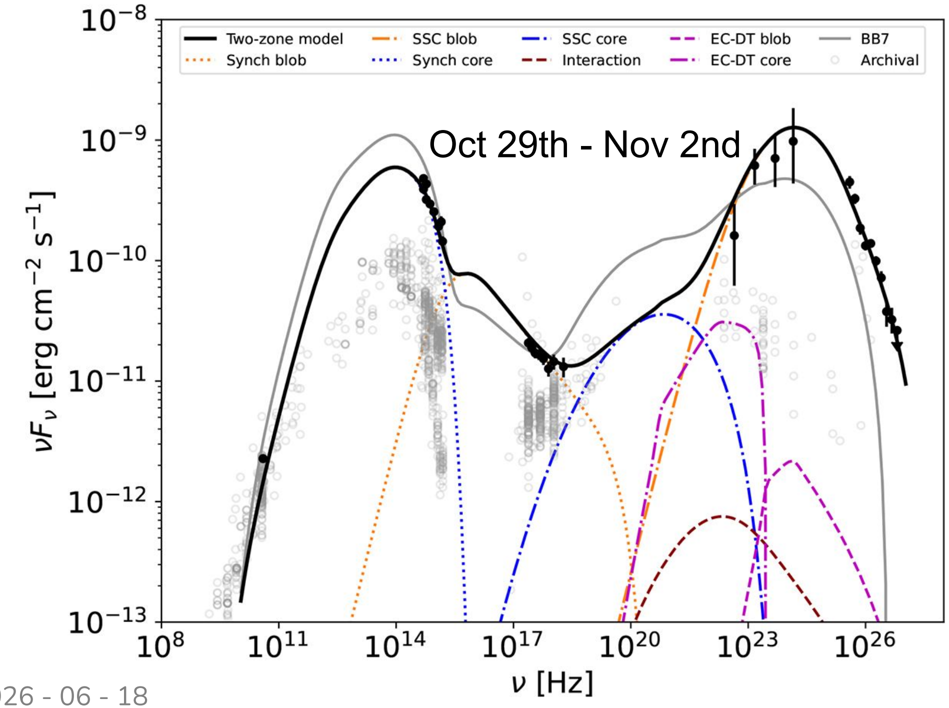

BL Lacertae 2022 flare K. Abe et al, A&A, 710, A41 (2026)

- Time-dependent modelling
  - 10 broadband SEDS identified bt Bayesian blocks
  - Leptonic scenarios (favored by IXPE results, I. Agudo et al. 2025)
    - One zone insufficient (SSC or EC) → Two-zone scenario with interaction
      - “Core” zone > “Blob” zone
    - Evolution of the flare driven by magnetic reconnection (min time scale variability)
      - “Blob” zone = newly formed plasmoid R = 3 x 10^{14} cm
      - Kept B, R, δ constant
      - Minimized changes in the “Core” zone

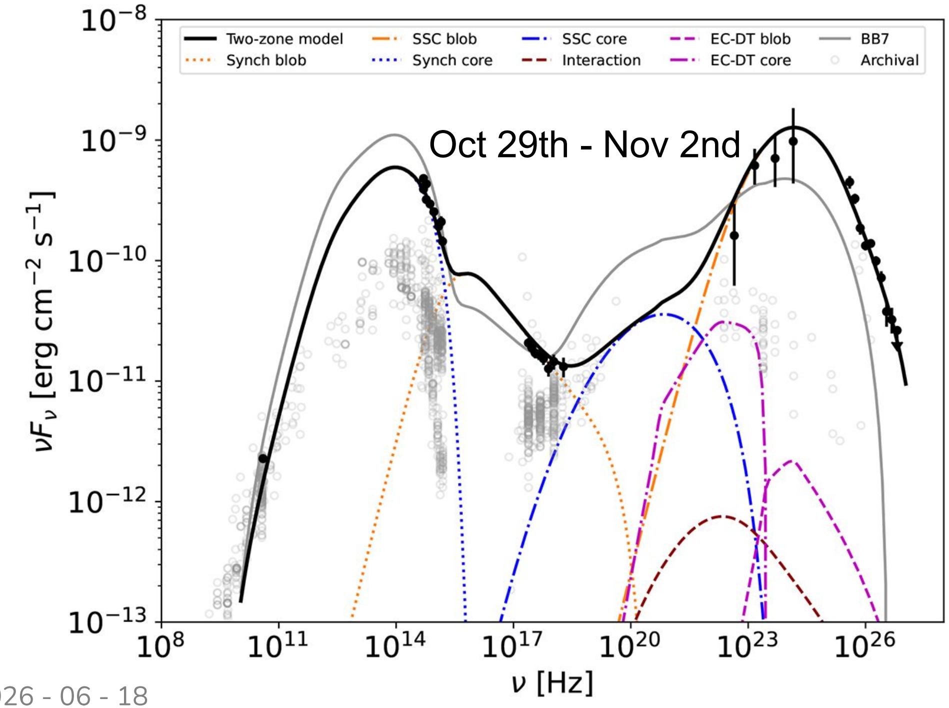

BL Lacertae 2022 flare K. Abe et al, A&A, 710, A41 (2026)

- Flare begins
  - Emission dominated by the core, up to X-ray energies
  - Gamma-ray emission: Plasmoids + EC scattering

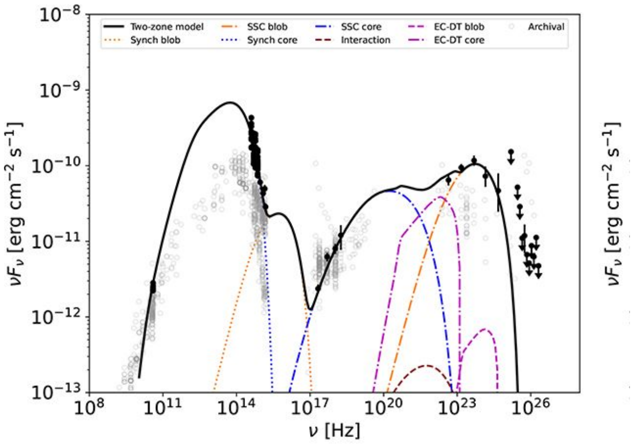

BL Lacertae 2022 flare K. Abe et al, A&A, 710, A41 (2026)

- Flare begins
  - Emission dominated by the core, up to X-ray energies
  - Gamma-ray emission: Plasmoids + EC scattering

- Magnetic reconnection progresses
  - Particles →higher energies →blob contributes to X-rays

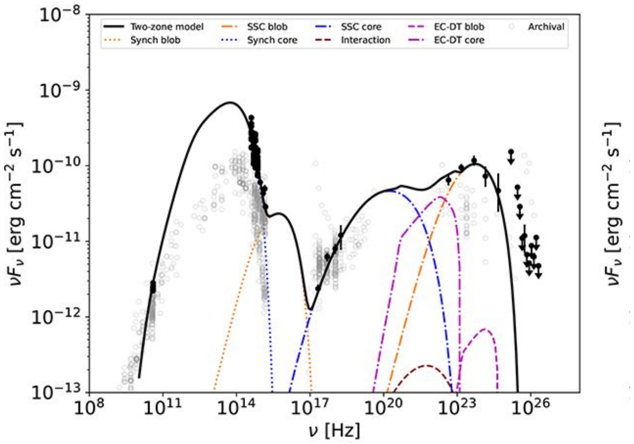

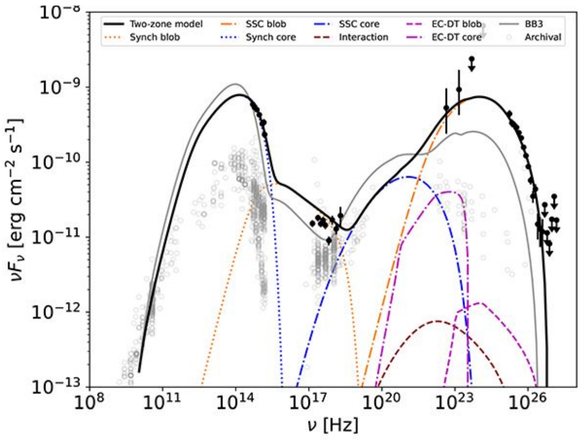

BL Lacertae 2022 flare K. Abe et al, A&A, 710, A41 (2026)

- Flare begins
  - Emission dominated by the core, up to X-ray energies
  - Gamma-ray emission: Plasmoids + EC scattering

- Magnetic reconnection progresses
  - Particles →higher energies →blob contributes to X-rays

- Several major ejections of plasmoid
  - Blob dominates the gamma-ray emission & at other wavelengths,
  - Each episode is followed by a relatively low-flux period

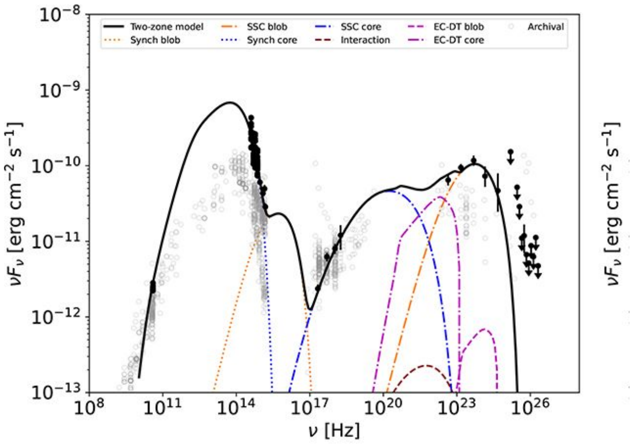

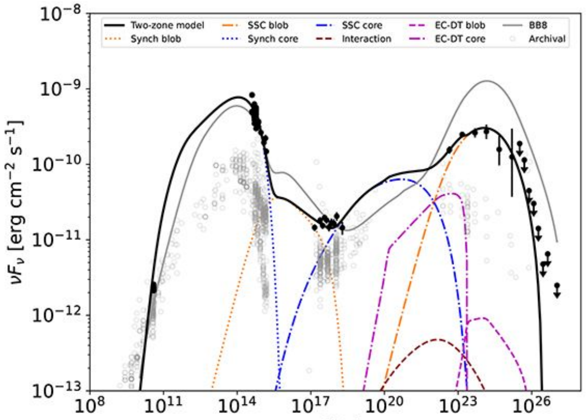

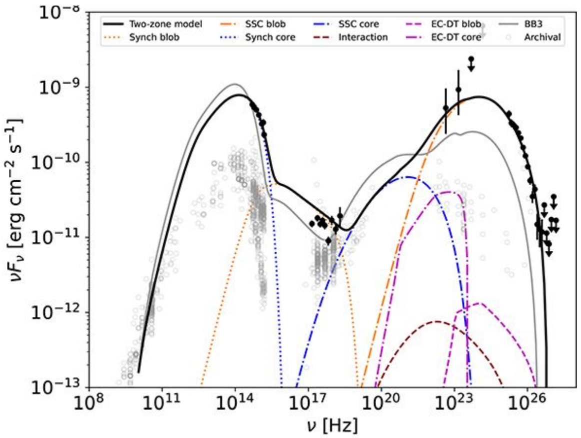

BL Lacertae 2022 flare

K. Abe et al, A&A, 710, A41 (2026)

- Primary driver of variability on day-to-week timescales
  - evolution of the particle populations, e.g. higher energies

- Primary driver of minutes time scale variability
  - Mini-jet scenario, also explains high δ

(1) Epoch	(2) Component	(3) γ_{min} $(\times 10^3)$	(4) γ_b $(\times 10^4)$	(5) γ_{max} $(\times 10^5)$	(6) n_1	(7) n_2	(8) B [G]	(9) K $[\times 10^{-2}\,cm^{-3}]$	(10) R $[\times 10^{15}\,cm]$	(11) Γ	(12) δ
BB7	Blob	2.70	1.05	1.00	2.7	3.6	0.50	3.00	0.3	33	33
	Core	0.30	0.23	0.07	2.2	3.3	0.20	0.01	100	20	20
BB8	Blob	4.00	1.00	3.80	2.1	3.8	0.50	7.50	0.3	33	33
	Core	0.30	0.18	0.07	1.9	3.0	0.20	0.01	100	20	20

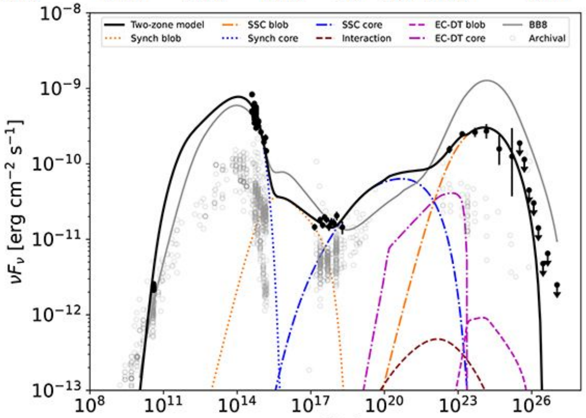

BL Lacertae 2022 flare

K. Abe et al, A&A, 710, A41 (2026)

- Primary driver of variability on day-to-week timescales
  - evolution of the particle populations, e.g. higher energies

- Primary driver of minutes time scale variability
  - Mini-jet scenario, also explains high δ

(1) Epoch	(2) Component	(3) γ_{min} ($\times 10^3$)	(4) γ_b ($\times 10^4$)	(5) γ_{max} ($\times 10^5$)	(6) n_1	(7) n_2	(8) B [G]	(9) K [$\times 10^{-2}$ cm^{-3}]	(10) R [$\times 10^{15}$ cm]	(11) Γ	(12) δ
BB7	Blob	2.70	1.05	1.00	2.7	3.6	0.50	3.00	0.3	33	33
	Core	0.30	0.23	0.07	2.2	3.3	0.20	0.01	100	20	20
BB8	Blob	4.00	1.00	3.80	2.1	3.8	0.50	7.50	0.3	33	33
	Core	0.30	0.18	0.07	1.9	3.0	0.20	0.01	100	20	20

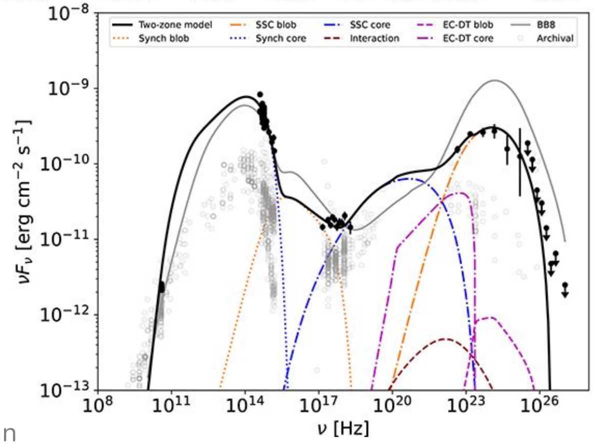

J. Otero Santos

G. Emery

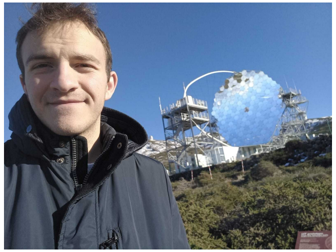

D. Cesarole

D. Morcuende

OP 313 discovery

K. Abe et al, accepted by A&A (2026), arXiv:2605.26681

- FSRQ type blazar at redshift z = 0.997

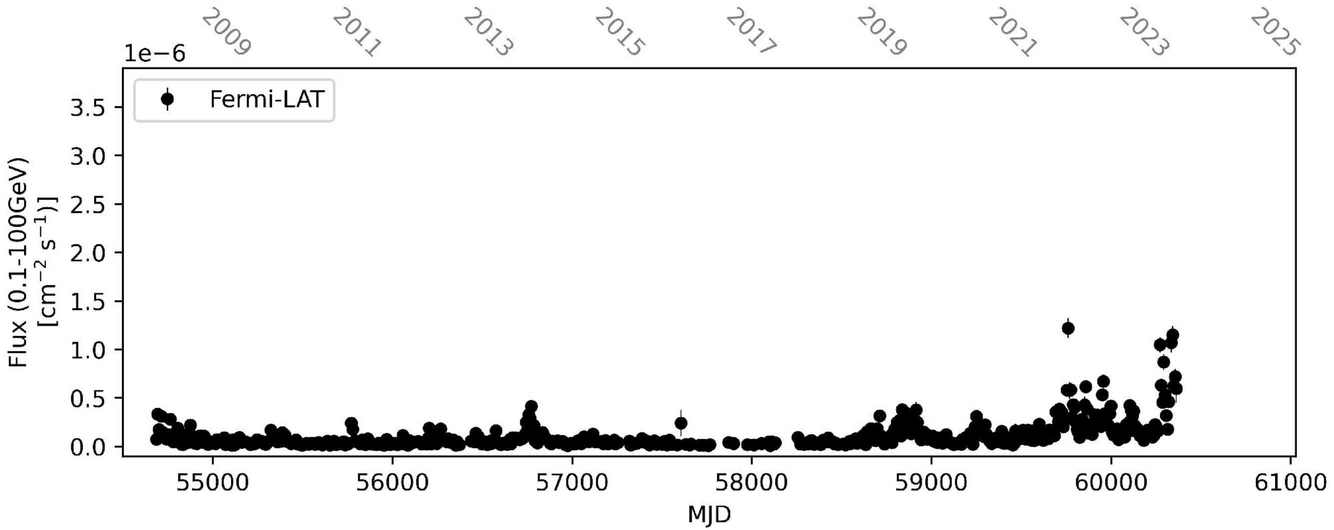

Adapted from the Fermi LAT Light Curve Repository (LCR)

OP 313 discovery

K. Abe et al, accepted by A&A (2026), arXiv:2605.26681

- FSRQ type blazar at redshift z = 0.997

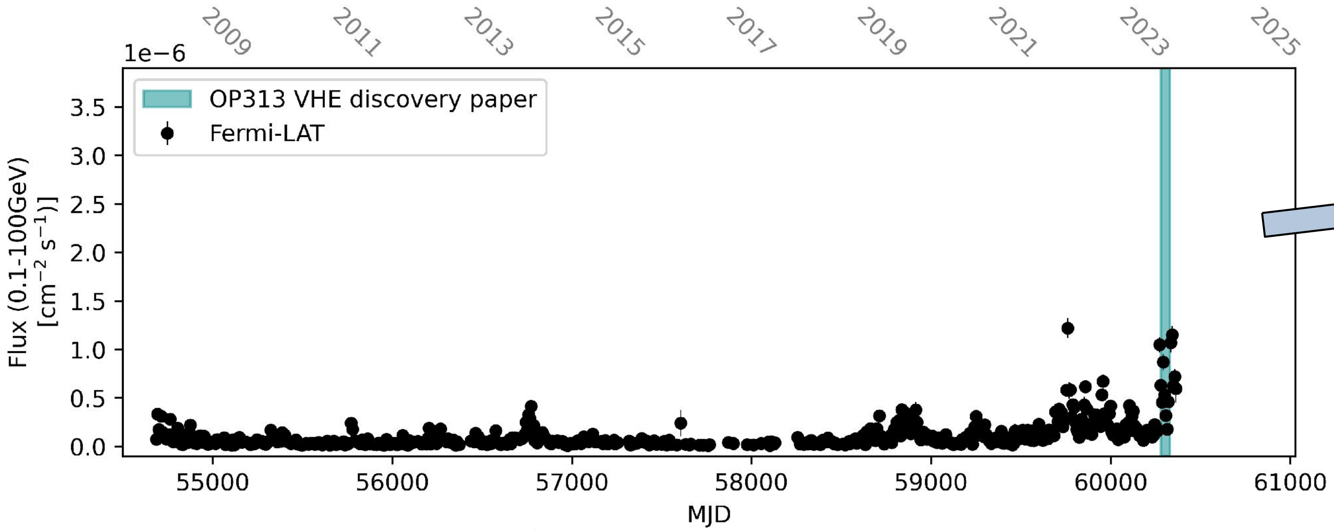

Adapted from the Fermi LAT Light Curve Repository (LCR)

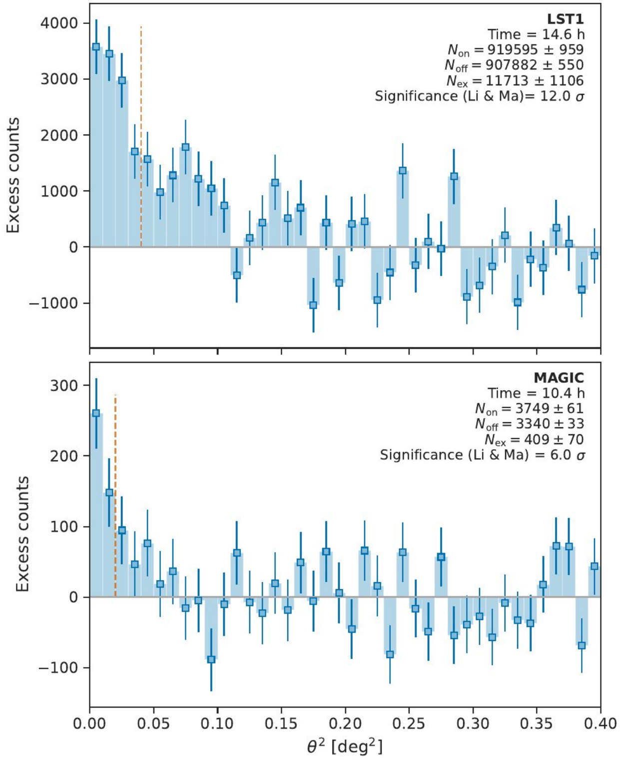

OP 313 discovery

K. Abe et al, accepted by A&A (2026), arXiv:2605.26681

- FSRQ type blazar at redshift z = 0.997

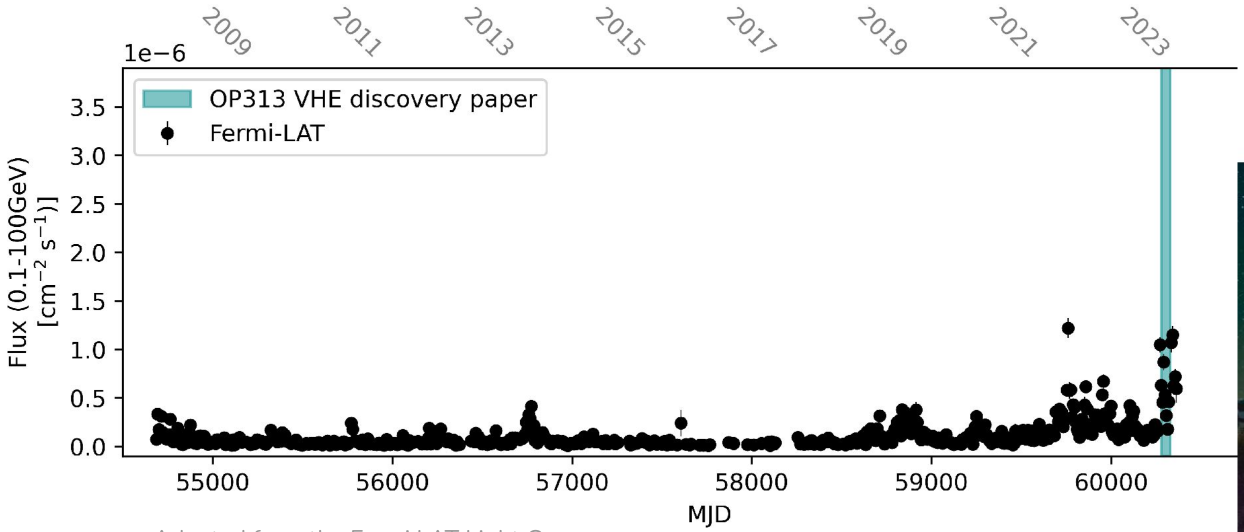

Adapted from the Fermi LAT Light Curve Repository (LCR)

→OP 313 became the 10th FSRQ and the most distant AGN detected at VHE gamma rays

OP 313 discovery

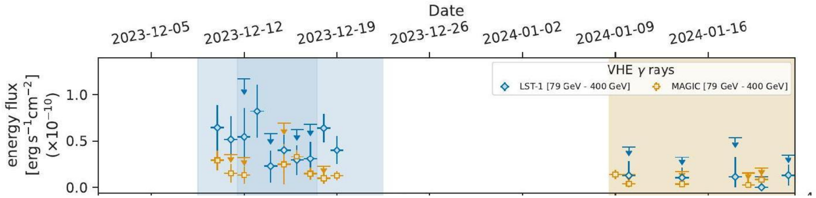

- Clear detection in VHE in December 2023
- Only upper limits in January 2024

OP 313 discovery

- Clear detection in VHE in December 2023
- Only upper limits in January 2024

- Rich MWL coverage
    - Flare accompanied by many other wavebands

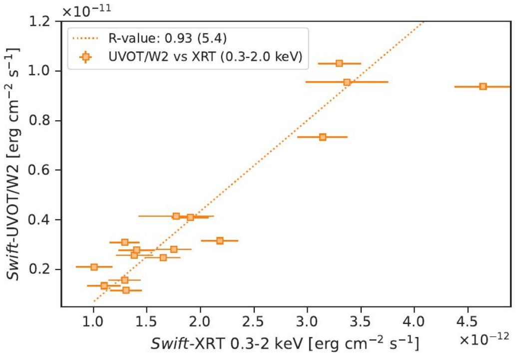

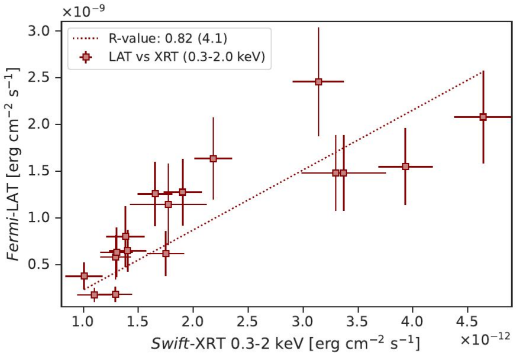

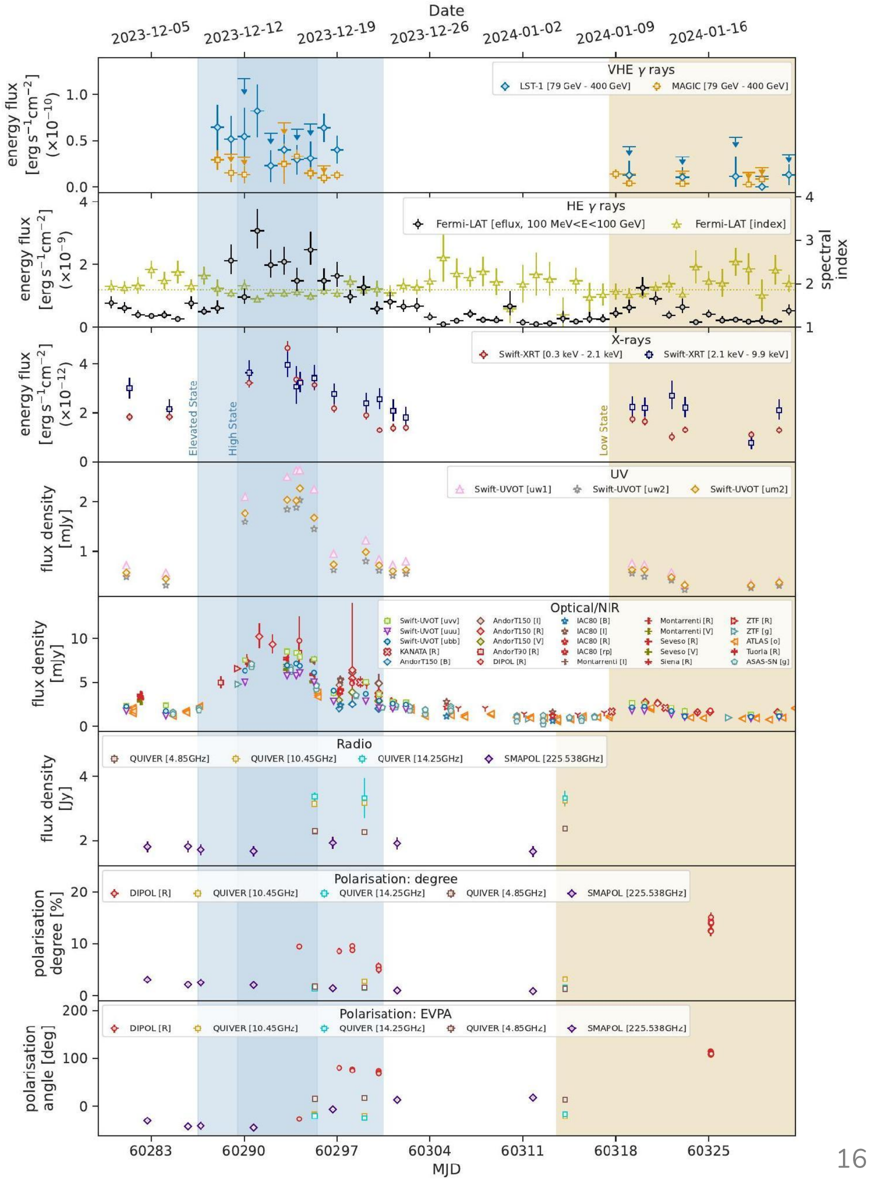

OP 313 discovery

K. Abe et al, accepted by A&A (2026), arXiv:2605.26681

- Leptonic model, two-zones (independent) necessary
- <u>Spectral-focused model</u>
  - Optimized to reproduce the SEDs
  - Stable "far" zone (radio, optical and partly X-rays)
  - Variable "near" zone (low-energy X-rays and gamma-rays)

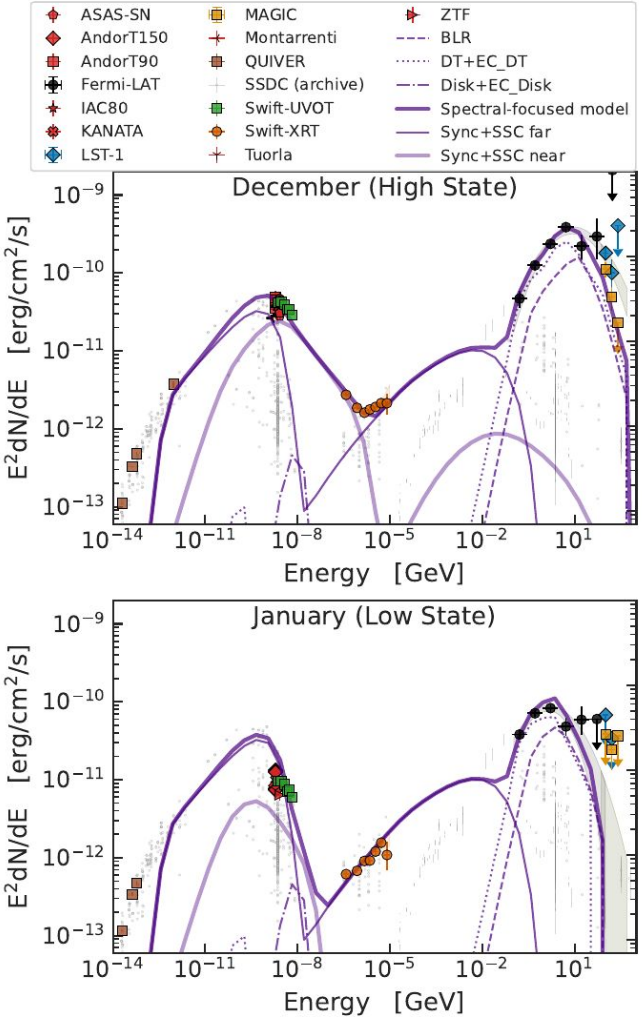

OP 313 discovery

K. Abe et al, accepted by A&A (2026), arXiv:2605.26681

- Leptonic model, two-zones (independent) necessary
- <u>Spectral-focused model</u>
  - Optimized to reproduce the SEDs
  - Stable “far” zone (radio, optical and partly X-rays)
  - Variable “near” zone (low-energy X-rays and gamma-rays)
    - Close to broad line region (BLR) → both BLR and dusty torus (DT) contribute to the external Compton (EC) emission
    - Doppler factor ≈100 required
    - Spectral index = 1.8 before/4.0 after the break (both states)
    - Changes between states explained by decrease in the electron break and maximum energy → cooling and injection driving the changes

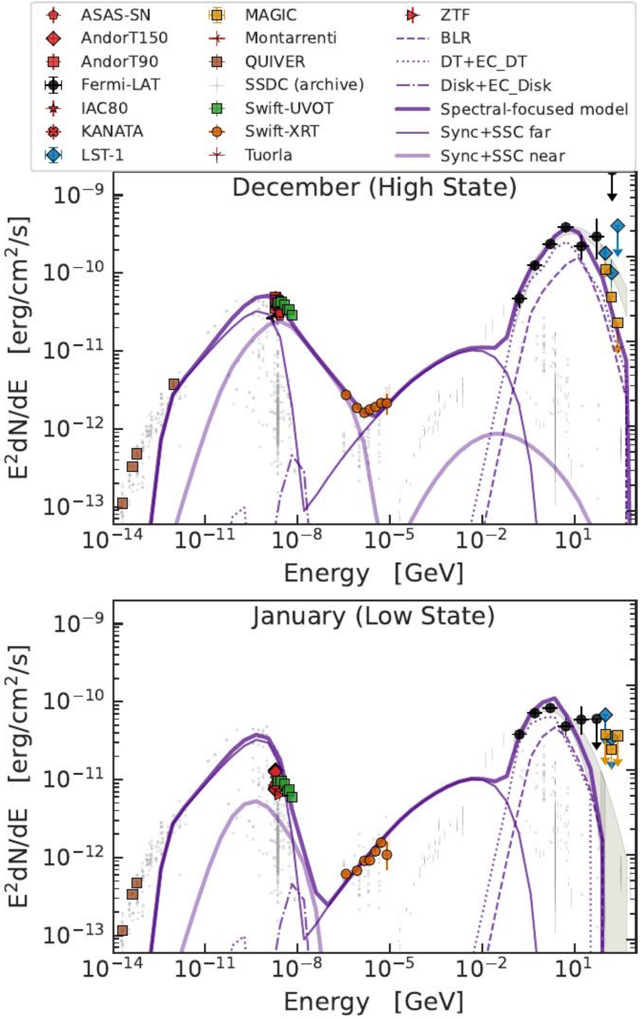

OP 313 discovery

K. Abe et al, accepted by A&A (2026), arXiv:2605.26681

- Leptonic model, two-zones (independent) necessary
- <u>Timing-focused model:</u>
  - Based on the identified MWL correlations
  - Stable “far” zone (radio)
  - Variable “near” zone (optical/UV to gamma-rays)

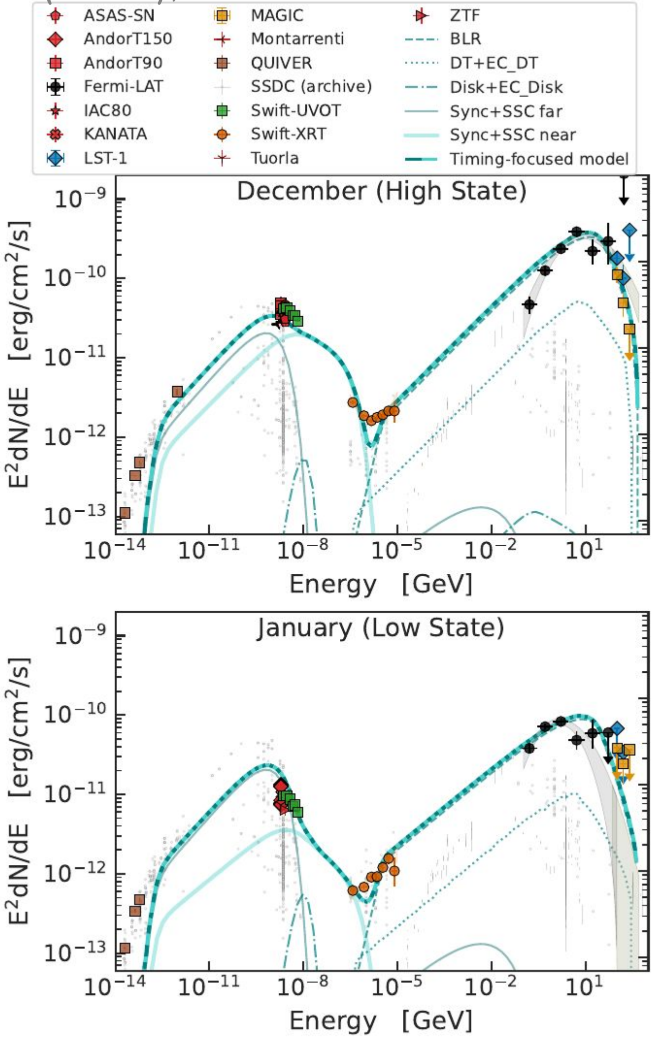

OP 313 discovery

K. Abe et al, accepted by A&A (2026), arXiv:2605.26681

- Leptonic model, two-zones (independent) necessary
- <u>Timing-focused model:</u>
  - Based on the identified MWL correlations
  - Stable “far” zone (radio)
  - Variable “near” zone (optical/UV to gamma-rays)
    - Well beyond the BLR
      → DT is the dominant target field for EC
    - Doppler factor ≈50
    - Spectral index = 2.2 before / 3.4 after the break (flare)
    - Changes between states explained by softening of the indices (2.4/3.7) & decrease in the electron break energy
      → cooling and injection driving the changes

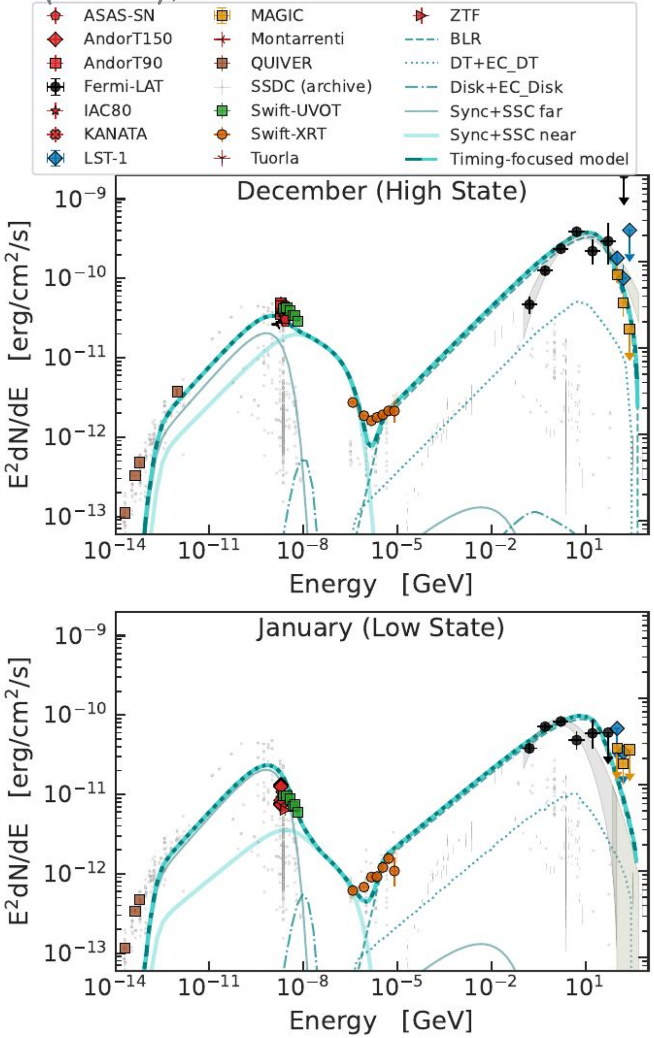

OP 313 discovery

K. Abe et al, accepted by A&A (2026), arXiv:2605.26681

- Red shift z=0.997 → strong absorption of gamma-ray by the extragalactic background light (EBL)
- Relation between observed and intrinsic flux

$$F_{obs} = e^{-\alpha \tau(z, E_{\gamma})} F_{intr}$$

- as a function of:
  - The optical depth for gamma-ray propagation $\tau(z, E_{\gamma})$
  - The scaling factor α

OP 313 discovery

K. Abe et al, accepted by A&A (2026), arXiv:2605.26681

- Red shift z=0.997 → strong absorption of gamma-ray by the extragalactic background light (EBL)
- Relation between observed and intrinsic flux

$$F_{obs} = e^{-\alpha \tau(z, E_\gamma)} F_{intr}$$

- as a function of:
  - The optical depth for gamma-ray propagation $\tau(z, E_\gamma)$
  - The scaling factor α

- Upper limits on α:
  - Baseline EBL model: Saldana-Lopez et al. (2021)
  - Assumed intrinsic spectrum as LP, LPEC, PLEC

→ $\alpha_{stat,95\%} < 1.14$

→ EBL density: $\lambda I_\lambda < 6.72$ nW m^2 sr^{-1} (λ = 0.6 μm)

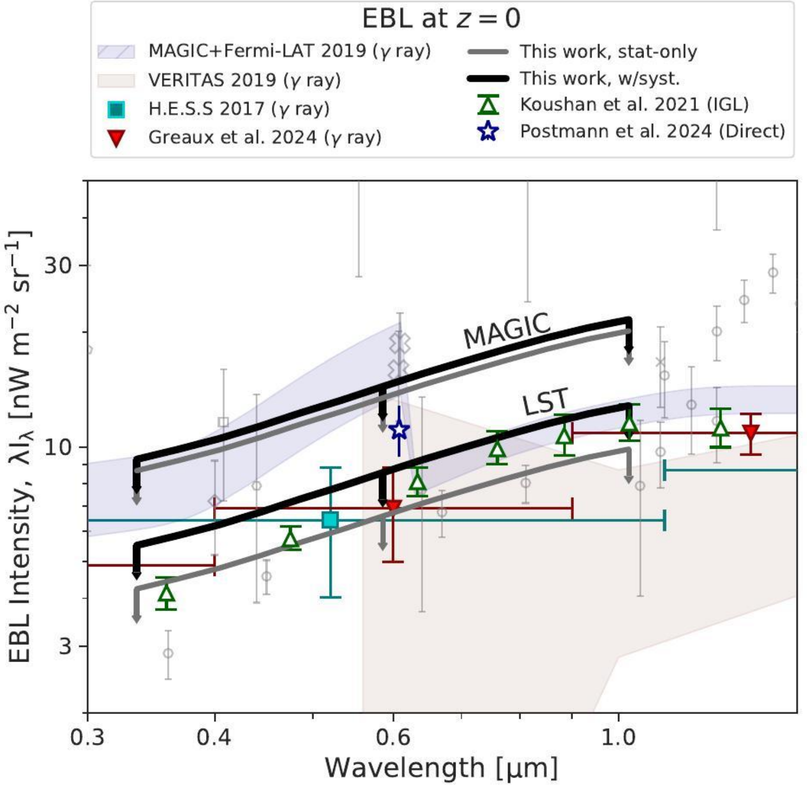

OP 313 discovery

K. Abe et al, accepted by A&A (2026), arXiv:2605.26681

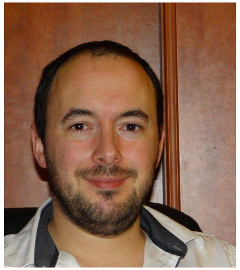

D. Sanchez

M. Nievas Rosillo

J. Otero Santos

D. Morcuende

A. Arbet-Engels

L. Heckmann

J. Baxter

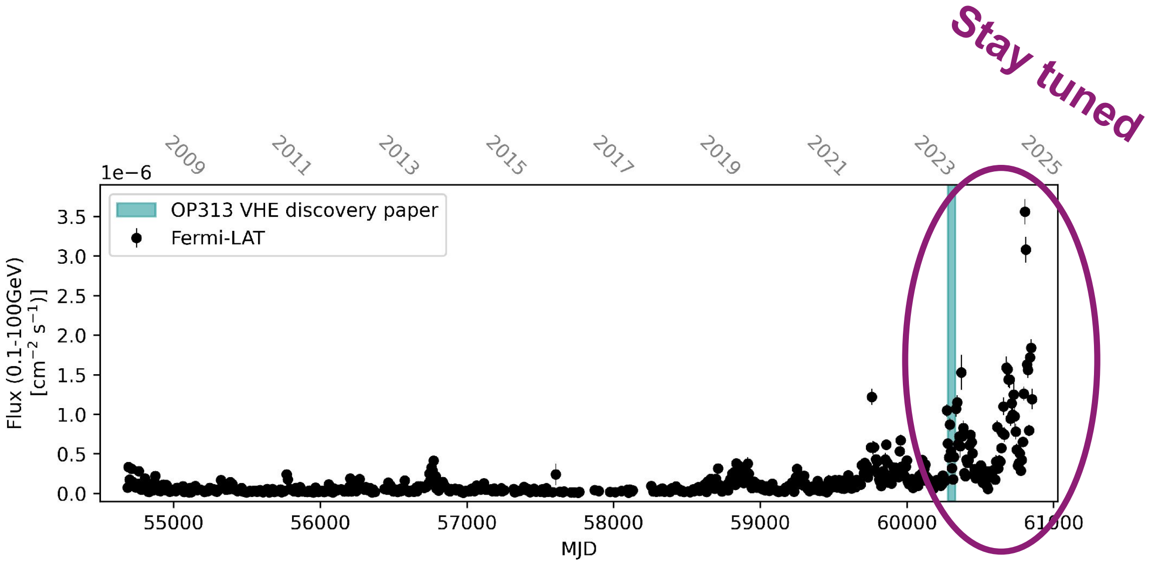

Adapted from the Fermi LAT Light Curve Repository (LCR)

Summary

- CTAO will expand the energy ranges accessible in the GeV/TeV with unprecedented sensitivity
- First glimpse with the science done by the LST-1 prototype covering a wide range of astrophysical sources
- LST's low energy threshold
  - pushes towards high-redshift blazars
  - Enables short-time variability studies with high precision

→ **More exciting science to come soon**

Thank you for your attention!

Credit: Irene Burelli

Back up

	Large-Sized Telescope (LST)
Energy range (in which sensitivity is optimized)	20 GeV – 150 GeV
Number of LST telescopes	4 (North)
Optical design	Parabolic
Primary reflector diameter	23.0 m
Effective mirror area (including shadowing)	370 m^2
Focal length	28 m
Total weight	103 t
Field of view	4.3 deg
Number of pixels	1855
Pixel size (imaging)	0.1 deg
Photodetector type	PMT
Telescope readout event rate after array trigger	>7.0 kHz
Telescope data rates (readout of all pixels; before array trigger)	24 Gb/s
Positioning time to any point in the sky (>30° elevation)	30 s
Pointing precision	<14 arcseconds
Observable sky	Any astrophysical object with elevation > 24 degrees